

Transition and self-healing process between chaotic and self-organized patterns observed during femtosecond laser writing

Nathaniel Groothoff,¹ Max-Olivier Hongler,² Peter Kazansky,³ and Yves Bellouard^{1,2,*}

¹Microsystems, Mechanical Engineering Dept., Eindhoven University of Technology (TU/e), Eindhoven, The Netherlands

²STI/IMT, Ecole Polytechnique Fédérale de Lausanne (EPFL), Lausanne, Switzerland

³ORC, University of Southampton, Southampton, UK

*yves@bellouard.eu

Abstract: We report evidence of intermittent behavior between chaotic and self-organized patterns while writing lines with a femtosecond lasers on the surface of a fused silica substrate. The patterns are accompanied by resolidified sub-microspheres and non-aligned grating lamellae. We observe that such dynamic behavior exhibits a striking similarity with the fluctuating content of a queuing system which alternate between random busy and idle periods.

©2015 Optical Society of America

OCIS codes: (050.6624) Subwavelength structures; (140.3390) Laser materials processing; (160.6030) Silica; (320.2250) Femtosecond phenomena; (320.7130) Ultrafast processes in condensed matter, including semiconductors.

References and Links

1. M. Birnbaum, "Semiconductor surface damage produced by Ruby lasers," *J. Appl. Phys.* **36**(11), 3688–3689 (1965).
2. J. Bonse, J. Krüger, S. Höhm, and A. Rosenfeld, "Femtosecond laser-induced periodic surface structures," *J. Laser Appl.* **24**(4), 042006 (2012).
3. R. Buividas, M. Mikutis, and S. Juodkazis, "Surface and bulk structuring of materials by ripples with long and short laser pulses: Recent advances," *Prog. Quantum Electron.* **38**(3), 119–156 (2014).
4. M. Beresna, M. Gecevičius, and P. G. Kazansky, "Ultrafast laser direct writing and nanostructuring in transparent materials," *Adv. Opt. Photonics* **6**(3), 293–339 (2014).
5. Y. Liao, J. Ni, L. Qiao, M. Huang, Y. Bellouard, K. Sugioka, and Y. Cheng, "High-fidelity visualization of formation of volume nanogratings in porous glass by femtosecond laser irradiation," *Optica* **2**, 329–334 (2015).
6. Y. Shimotsuma, P. G. Kazansky, J. Qiu, and K. Hirao, "Self-organized nanogratings in glass irradiated by ultrashort light pulses," *Phys. Rev. Lett.* **91**(24), 247405 (2003).
7. F. Liang, R. Vallée, and S. L. Chin, "Mechanism of nanograting formation on the surface of fused silica," *Opt. Express* **20**(4), 4389–4396 (2012).
8. A. Champion, M. Beresna, P. Kazansky, and Y. Bellouard, "Stress distribution around femtosecond laser affected zones: Effect of nanogratings orientation," *Opt. Express* **21**(21), 24942–24951 (2013).
9. J. Canning, M. Lancry, K. Cook, A. Weickman, F. Brisset, and B. Poumellec, "Anatomy of a femtosecond laser processed silica waveguide [Invited]," *Opt. Mater. Express* **1**(5), 998–1008 (2011).
10. A. Champion and Y. Bellouard, "Direct volume variation measurements in fused silica specimens exposed to femtosecond laser," *Opt. Mater. Express* **2**(6), 789–798 (2012).
11. P. G. Kazansky, M. Beresna, M. Gecevičius, C. Corbari, Y. Shimotsuma, M. Sakakura, K. Miura, K. Hirao, and Y. Bellouard, "Phase transitions induced by ultrafast laser writing in transparent materials," in *Conference on Lasers and Electro-Optics: Laser Science to Photonic Applications, CLEO, Baltimore, MD* (OSA, 2011).
12. J. Medhi, *Stochastic Models in Queueing Theory*, 2nd Edition (Academic, 2002).
13. C. Hnatovsky, R. S. Taylor, E. Simova, V. R. Bhardwaj, D. M. Rayner, and P. B. Corkum, "Polarization-selective etching in femtosecond laser-assisted microfluidic channel fabrication in fused silica," *Opt. Lett.* **30**(14), 1867–1869 (2005).
14. S. Rajesh and Y. Bellouard, "Towards fast femtosecond laser micromachining of fused silica: The effect of deposited energy," *Opt. Express* **18**(20), 21490–21497 (2010).
15. S. Richter, M. Heinrich, S. Döring, A. Tünnermann, S. Nolte, and U. Peschel, "Nanogratings in fused silica: Formation, control, and applications," *J. Laser Appl.* **24**(4), 042008 (2012).
16. D. Vipparty, B. Tan, and K. Venkatakrishnan, "Nanostructures synthesis by femtosecond laser ablation of glasses," *J. Appl. Phys.* **112**(7), 073109 (2012).

17. J. Siegel, D. Puerto, W. Gawelda, G. Bachelier, J. Solis, L. Ehrentraut, and J. Bonse, "Plasma formation and structural modification below the visible ablation threshold in fused silica upon femtosecond laser irradiation," *Appl. Phys. Lett.* **91**(8), 082902 (2007).
18. A. Mermillod-Blondin, J. Bonse, A. Rosenfeld, I. V. Hertel, Y. P. Meshcheryakov, N. M. Bulgakova, E. Audouard, and R. Stoian, "Dynamics of femtosecond laser induced voidlike structures in fused silica," *Appl. Phys. Lett.* **94**(4), 041911 (2009).
19. J. Reif, O. Varlamova, and F. Costache, "Femtosecond laser induced nanostructure formation: self-organization control parameters," *Appl. Phys., A Mater. Sci. Process.* **92**(4), 1019–1024 (2008).
20. "HPFS Fused Silica Standard Grade - Product Information Sheet" (Corning Incorporated, 2008).
21. J. F. Shackelford and W. Alexander, *CRC Materials Science and Engineering Handbook*, 3rd ed. (CRC Press, 2000).
22. G. Urbain, Y. Bottinga, and P. Richet, "Viscosity of liquid silica, silicates and alumino-silicates," *Geochim. Cosmochim. Acta* **46**(6), 1061–1072 (1982).
23. Y. Bellouard, E. Barthel, A. A. Said, M. Dugan, and P. Bado, "Scanning thermal microscopy and Raman analysis of bulk fused silica exposed to low-energy femtosecond laser pulses," *Opt. Express* **16**(24), 19520–19534 (2008).
24. T. Kumada, H. Akagi, R. Itakura, T. Otobe, and A. Yokoyama, "Femtosecond laser ablation dynamics of fused silica extracted from oscillation of time-resolved reflectivity," *J. Appl. Phys.* **115**(10), 103504 (2014).
25. W. Weibull, "A statistical distribution function of wide applicability," *ASME J. Appl. Mech.* **18**, 293–297 (1951).

1. Introduction

Under certain exposure conditions, periodic patterns have been created both on the surface and in the bulk of various materials following pulsed, polarized laser irradiation [1–5] (and references therein). For ultrashort pulsed lasers, it is possible to obtain periodicities smaller than the wavelength of irradiation in transparent material. Intriguingly, the pattern seemingly stems from a self-organized phenomena [6].

Some of the proposed ideas regarding the formation of the periodic patterns, or nanogratings, have been through the interference of the laser radiation and the induced electron plasma [6] or through a nanoplasmonic model and incubation phenomena [7]. Even though some uncertainty surrounds the formation of the structures, it is apparent that there is an accompanying stress profile that forms within and around the nanogratings [8]. Evidence of porous material within the nanogratings [9], combined with experimental observations of volume expansion [10] suggest that there is essentially compressive stress formation outside, but in very close proximity to the laser affected zones.

The observations within this report, show a transition between a periodic pattern with nanograting like properties and a chaotic pattern, in an exposure regime (pulse duration > 200 fs and in a non-cumulative regime) where the formation of continuous modifications is excluded. Previous reports of the transition between nanogratings and a damage region [11] showed a single transition to nanogratings within the laser written track. Once the transition had taken place, the modification was deemed to be in a more energy stable regime and the reverse transition was excluded. Landau theory was applied to offer an explanation for the transition. However, a similar transition reported here shows a clear disparity with that explanation, such that the transition can occur multiple times and hence neither modification regime is of a lower energy state than the other. The transition from the chaotic pattern to the self-organized could be considered a self-healing process and is most likely linked with the evolution of stress in the glass.

For the same irradiation conditions, there are generally two outcomes, self-organized or chaotic patterns. This shows a close analogy with a queueing system [12], whereby quanta of deposited energy constitutes the customer and the process of energy dissipation, the server. This phenomenological idea, its mathematical formulation and its overall predictive potential is presently under investigation.

This paper will present the experimental results of the pattern transitions and particular features of laser modification. A proposed mechanism of the formation of the chaotic region linked to stress will be presented.

2. Experimental observations of intermittent behavior

2.1 Experimental method

Using an Amplitude Systèmes' femtosecond laser with a pulse duration of ~ 270 fs and a wavelength of 1030 nm, lines were written to intersect the surface of silica glass (Corning 7980 UV HPFS). The repetition rate of the laser was 400 kHz and the writing speed was varied to achieve the desired energy deposition, or dosage, using high precision linear translation stages (PI Micos GmbH). The conditions of exposure were set by fixing the range of energy depositions (dosage) between 2 and 10 J/mm² for pulse energies of 180, 200 and 220 nJ that had previously been identified as likely to produce the most interesting results for the nanogratings. The corresponding number of overlapping pulses is 25 – 124 for 180 nJ, 22 – 112 for 200 nJ and 20 – 102 for 220 nJ. The laser was focused onto the specimen using a 40X objective lens (OFR/Thorlabs) that had an NA of 0.4 creating a maximum modification width of approximately 1.5 – 2.0 μm as observed by the scanning electron microscopy (SEM) imaging. By inclining the laser track to the surface of the specimen by $\leq 1^\circ$, the modification was ensured to cross the surface even if slight misalignment of the focal spot to the surface plane occurs (Fig. 1). This first method also allowed the rapid observation of the material modification - the Laser Affected Zone (LAZ) - for different levels of writing depth, in the direction of laser propagation and without polishing the surface or writing multiple laser tracks at varying depths.

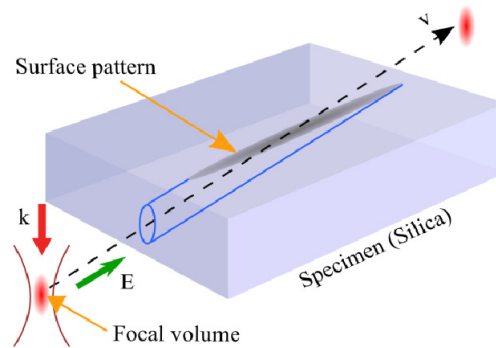


Fig. 1. Schematic of the laser processing indicating the scanning direction (v), the laser's irradiation direction (k), the focal volume that modifies the material, the pattern that is written on the surface and the polarization (E), which is parallel to the laser-writing direction. The blue solid lines indicate the passage of the laser focal volume through the substrate.

While the inclined laser track provides the opportunity to study the resultant laser affected zone at different cross-sections in the propagation direction, it does however impose a limitation, when directly comparing the modification over the entire laser track, since exposure conditions are not rigorously identical across the length of the laser track (i.e. the volume of exposed material varies). To overcome this issue, we have also written laser tracks parallel to the surface, i.e. in-plane, and to avoid the issue of misalignment perpendicular to the surface, a number of tracks were written at various heights (above and below) the surface. The laser focal volume began off the specimen crossing the top edge and continuing to a length of 8 mm. The tracks that were studied were those that were created from the center part of the LAZ in the propagation direction.

Following the laser writing, a specimen was chemically etched for ~ 5 minutes in aqueous hydrofluoric acid (concentration 2.5%) to reveal the surface modification patterns of the nanograting lamellae that have been found to etch at a higher rate than the surrounding material [13,14]. Prior to imaging with a scanning electron microscope (FEI Quanta 600) a

thin coating (≤ 30 nm) of gold was sputter-coated to create a conductive surface and avoid surface charging that can be induced by the electron microscope.

2.2 Surface modification

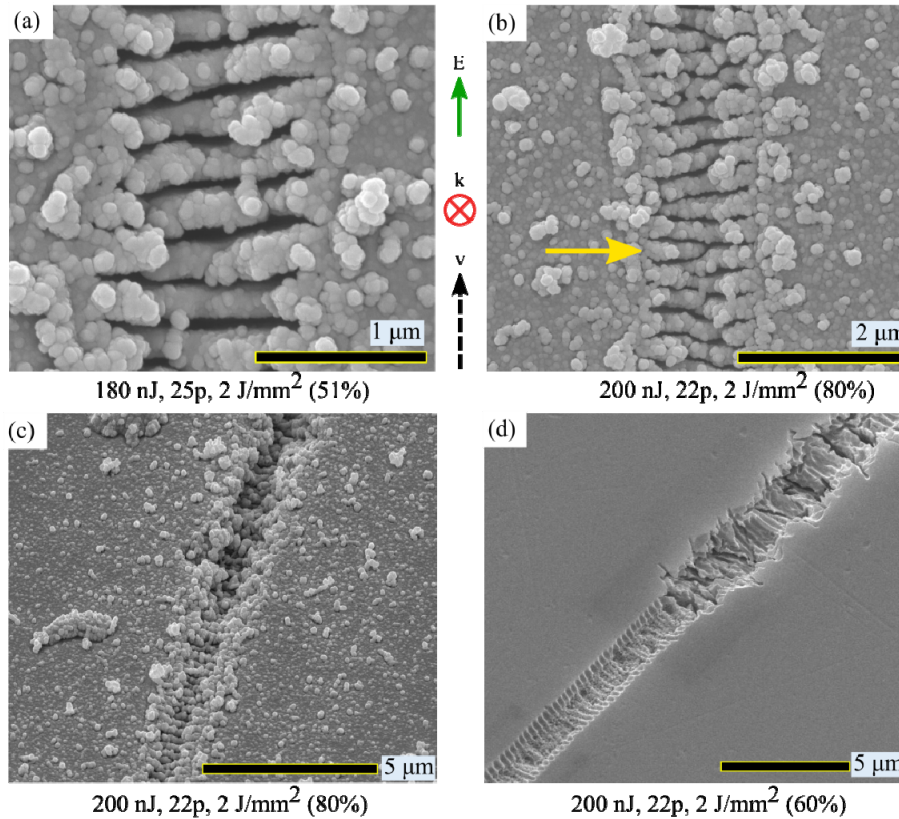


Fig. 2. SEM images of (a) unetched self-organized pattern for 180 nJ pulse energy, (b) unetched self-organized pattern for 200 nJ pulse energy also indicating the irregularity in lamellae formation (orange arrow), (c) and (d) the transition to chaotic from self-organized for both an unetched and etched specimen, respectively. The labels below each image refer to pulse energy, number of overlapping pulses, the energy deposited and the percentage of focal volume below the surface.

The surface of an un-etched specimen was examined using the SEM to reveal the raw laser modification patterns. A couple of the laser tracks were imaged (Fig. 2) that corresponded to those that were etched and revealed the most interesting features. The nanograting structures (Fig. 2(a) and 2(b)) show that the lamellae are present but covered in a form of particulates. These particulates are spherical in nature and are likely to be re-solidified silica originating from molten silica that accompanied minor ablation. With a lower magnified image, a debris field can be seen surrounding the laser tracks (Fig. 2(c)) that further provides evidence that minor ablation has occurred. Interestingly there is a similarity between the spherical particulates found on the surface of the unetched specimens to that of the etched specimen (Fig. 3 and Fig. 4) leading to the idea that both processes are related. The spherical particulates of the etched structures will be discussed in a later section.

The uniformity of the lamellae of the nanogratings is not consistent, as can be seen in Fig. 2(b) by the orange arrow, which poses a question into the underlying formation mechanism of the nanogratings. If they do in fact form through a self-organized phenomenon that involves interference, it would be reasonable to expect that the interference creates a regular and

uniform pattern, which for the most part, is observed with the nanogratings. However, there are occasions when this uniformity is disturbed for both the actual lamellae and the material in between. Unsurprisingly, the non-uniformity of the lamellae is replicated with the etched specimen, consistent with principle that the etching process attacks the porous lamellae preferentially over the other features of the nanogratings.

2.3 Self-organized patterns

A post-etched specimen was examined using the SEM. Concentrating on the self-organized parts of the nanogratings, a collection of images for different number of overlapping pulses (energy deposition) but the same pulse energy was produced (Fig. 3). Even though the volume percentage of the LAZ that was beneath the surface varied, the self-organized nanogratings presented in Fig. 3 represent the self-organized nanogratings found along the particular laser track. The periodicity of the self-organized patterns decreases as the number of pulses increases in-line with the observation by Shimotsuma *et al.* [4] and subsequently by Richter *et al.* [15] and Liang *et al.* [7]. In addition to the reduced periodicity, the uniformity of the periodicity has also changed; higher energy deposition causes the lamellae to be discontinuous laterally across the modification zone. Liang *et al.* [7] offers the explanation that new lamella are created adjacent to existing lamella with further pulse irradiation due to the incubation effect whereby the threshold for lamellae development is reduced enabling more lamella to be created. This then would imply that the images shown in Fig. 3 are an evolutionary picture of the last nanograting structure (112 pulses), such that the material is somewhat malleable with the femtosecond laser passing through various structures during exposure.

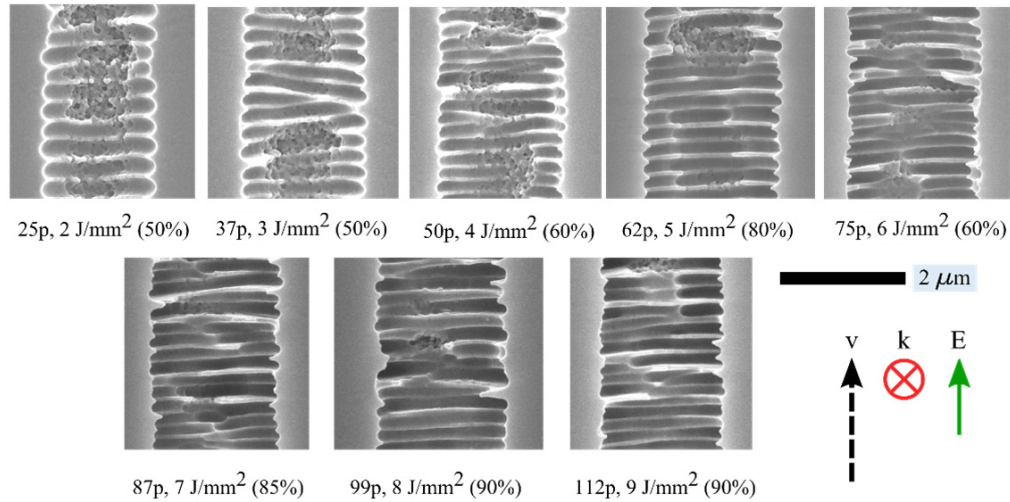


Fig. 3. A comparison of the self-organized nanogratings for different energy depositions from a pulse energy of 180 nJ. The labels below the image represent the number of overlapping pulses, energy deposition and the volumetric percentage of the LAZ below the surface.

As mentioned in Section 2.2, accompanying some of the self-organized patterns was the formation of sub-microspherical particulates within the modification track. The origin of the particulates is almost definitely thermal and might be a precursor step before ablation and jetting of these submicron particles that was observed on the unetched specimen and in [16]. To support this argument, we first note that evidence of partially molten interfaces is found in the center of the track where the energy deposition is the highest (Fig. 4(a)). The mechanism of submicron particles formation seems to occur after the former of self-organized structures and resembles in this case, a liquid-interface breaking due the temperature rising above the

critical point. Further supporting a thermal origin, logically more sub-microspheres are generated with higher pulse energy (Fig. 4(b)). Interestingly, as can be seen in Fig. 4(c), the nanogratings structure is clearly visible on the sides of the track. It further supports the hypothesis of a liquid-air interface that first ruptures from the middle and propagates sideways. It also shows that the sub-microsphere production process takes place after the nanogratings formation and well after the laser exposure.

Typical timescale for the modification of silica following femtosecond laser excitation are on the order of tens of nanoseconds. Siegel *et al.* [17] reported that the material excitation and ablation process on the surface of fused silica had finished after 10 ns. And a bulk fused silica study concluded that modifications induced by femtosecond pulses had stabilized by a similar time frame [18]. Figure 4(d) shows that increasing the pulse energy to 200 nJ from 180 nJ has resulted in more sub-microspheres in the laser track for the same energy deposition (2 J/mm^2). To achieve the same energy deposition with 200 nJ/pulse as for 180 nJ/pulse, the number of overlapping pulses was reduced to 22 from 25. Thus the formation of the sub-microspheres is strongly linked to the pulse energy rather than the number of overlapping pulses i.e. energy deposition. This means that the formation of the nanogratings is an energy deposition effect but the formation of the sub-microspheres is from the individual pulses. The sizes of the sub-microspheres range between 50 – 100 nm as measured from the SEM images (Fig. 4).

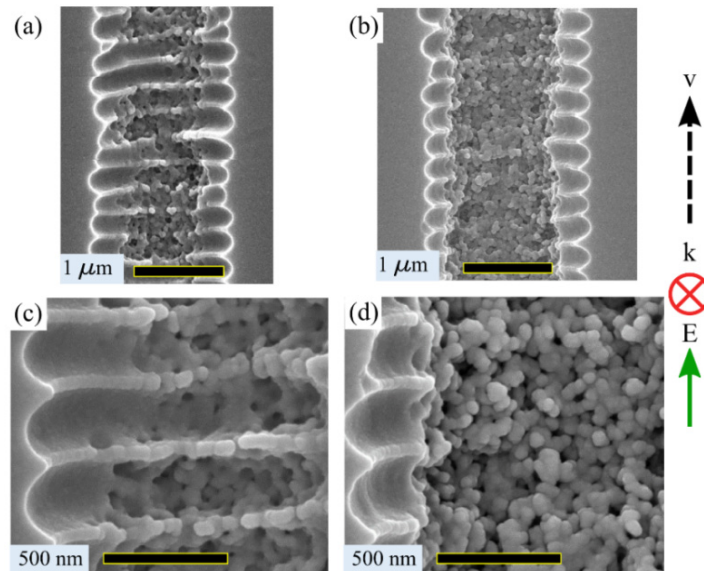


Fig. 4. Sub-microspheres in the center of the laser patterns. (a) 180nJ, 25 pulses, 2 J/mm^2 , 35% of laser affected zone (LAZ) below surface; (b) 200nJ, 22 pulses, 2 J/mm^2 , 50% of LAZ below surface. (c) Magnified image of the nanospheres for 180 nJ, 2 J/mm^2 (different position from (a)) and (d) magnified image of 200nJ, 2 J/mm^2 .

Similar sub-microspheres were observed by Reif *et al.* [19] when exposing the dielectric CaF_2 to 5000 circular polarized pulses with a wavelength of 800 nm and 120 fs pulse duration creating a peak intensity of $8 \times 10^{12} \text{ W/cm}^2$. In comparison, the 3 J/mm^2 specimen reported here received a peak intensity of $\sim 2.6 \times 10^{13} \text{ W/cm}^2$, linear polarization and was subject to only 33 pulses.

Melting of fused silica doesn't occur at a specific temperature as opposed to ice for example, but rather undergoes a gradual change in viscosity eventually reaching a similar value to that of water (1 Pa.s). Nevertheless certain temperatures associated with material phases of silica have been identified based on the viscosity of the silica at those temperatures.

For example, Corning 7980 UV HPFS fused silica has a softening point at 1600 °C [20], which is similar to the “melting” temperature as specified in [21]: 1710 °C. The liquid state of silica was still apparent at temperatures around 2400 °C [22] meaning that this temperature would need to be exceeded to reach a vapor phase. A basic estimate of the silica’s temperature induced by laser excitation can be determined using the relationship $\Delta T = E_{dep}/\rho \cdot C_p$, where E_{dep} is the volumetric laser energy deposition per pulse (i.e. energy deposition per unit volume), ρ is the solid density 2200 kg/m³ and C_p is the specific heat capacity of fused silica 740 J/kg/K. For a pulse energy of 180 nJ contained within a volume of 31.4 μm^3 (an affected zone of diameter 2 μm and depth of 10 μm ; producing a volumetric energy deposition of $5.7 \times 10^9 \text{ J/m}^3$) assuming the affected zone has a cylindrical shape and all of the energy is converted to electronic excitation, the temperature is $\sim 3520 \text{ K}$ (3250 °C). This value is 850 K above the vaporization temperature mentioned above (2400 °C).

However, the dynamics of laser excitation and subsequent material response may not be entirely comparable to that of regular material phase transitions from thermal excitation. Rather than atomic bond excitation that occurs from thermal excitation, the laser field directly excites electronic states. This excitation leads to additional electronic excitation that in turn thermally excites the material locally that can subsequently cause ablation. Thus a question that is raised is when is the material in a liquid like state? Presumably there is a temperature gradient extending from the center of the laser modification zone outwards to the unexcited material and that this gradient is very steep, somewhere in the range of 1000 K/ μm presuming that the center of the LAZ is at or above 2000 K. There can be a few sources of the sub-microspheres originating from the silica melt – either a solidification of the ablated material that isn’t ejected far from the laser track, or solidification of a melt that was not in a state for ablation. Although it is not entirely clear which pathway the material may have formed from, it is clear that there has been some form of localized melting.

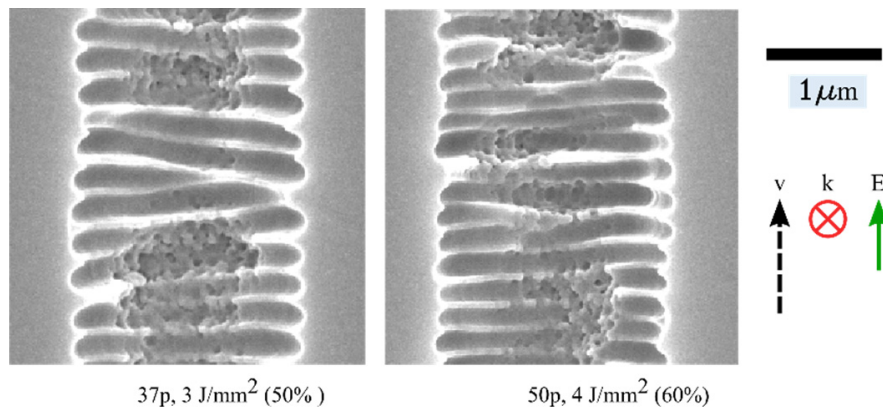


Fig. 5. Adjacent lamellae overlap each other. Pulse energy was 180 nJ and the image label refers to the number of pulses, energy deposition and the percentage volume of the LAZ below the surface.

Another interesting observation is the fact that some of the lamellae aren’t parallel or uniform in the positioning as eluded to earlier. In some cases, the self-organized nanogratings expressed a tendency for the lamellae to overlap forming a non-parallel structure. This is not to be confused with the disordered structure. The angle of the 180 nJ, 37 pulses (3 J/mm^2) lamellae (Fig. 5 *left*) rotates from the horizontal (0°) to approximately $+5.5$ degrees but then undergoes a sharp change to -8.5 degrees with respect to the initial angle of the lamellae (bottom of the figure). The nanograting structure is still present but the alignment of the lamellae is no longer uniform. Should the argument of interference be true in the formation of

the nanogratings, then it would be apparent that the interference is dynamic or there are multiple competing interferences.

The dynamic nature could alternatively be driven by changes in the polarization state of the irradiation, although it is unusual that the change affects individual lamellae. Considering the number of pulses that have irradiated the 3 J/mm^2 track (Fig. 5 *left*) is 37 and that the formation of the nanogratings is a cumulative process, it would be reasonable to expect that there would be a transition to the different angle; a blending between the different angles even if the change in polarization was sudden. This is just one possibility, other explanations could be proposed. At this stage, there is no clear understanding for this lack of uniformity in the nanogratings lamellas alignment.

2.4 Evidence of intermittent behavior: self-healing process

The creation of chaotic structures with the same exposure conditions for producing the nanogratings was found to occur at random locations along the laser tracks. The transitions occur abruptly and in both forms; from chaotic to self-organized and vice-versa. Figure 6 shows various SEM images of the different transitions. A single transition from chaotic to self-organized is displayed in Fig. 6(a), where the lengths of either section exceed $50 \mu\text{m}$. This highlights that persistent structures can exist. However, it was also observed that within a self-organized nanograting track the chaotic structure can suddenly form (Fig. 6(b)). This situation was also evident in the chaotic track where short sections self-organized nanogratings can be surrounded by chaotic structures as shown in Fig. 6(c).

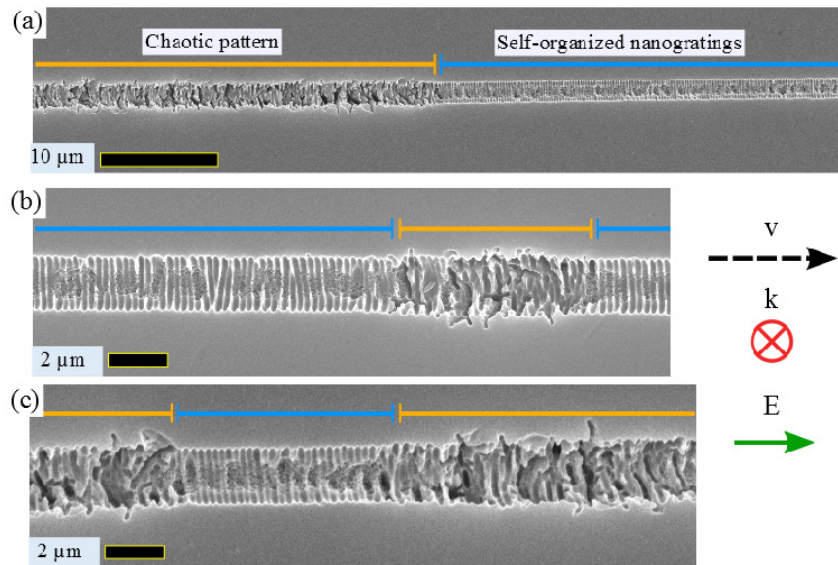


Fig. 6. (a) Transition to self-organization with both self-organized and chaotic patterns extending more than $50 \mu\text{m}$ in either direction, (b) a chaotic pattern between self-organization, and (c) the alternative case of a short section ($\sim 10 \mu\text{m}$) of self-organization located between the chaotic patterns.

Images at the location of the transitions between the different structures are shown in Fig. 7. Here it is apparent that the chaotic structure contains cracks; which are enlarged by the HF etching process producing smooth ends. This provides strong evidence that the chaotic structures are formed due to stress. We note that the cracks are preferably oriented perpendicular to the writing direction. Previous evidence and discussion about crack formation associated with nanogratings was given by Bellouard *et al.* [23]. Differentiating the results presented here is the cracks are present in the chaotic structures rather than in the self-

organized nanogratings. The transition back to the self-organized structure can be viewed as self-healing process where the self-organized structure once again takes precedence.

What is unexpected from these observations is that both the localized melting/resolidification occurring at the center portion of the laser track are directly adjacent to the disordered structures. Melting would normally allow for stress abatement or prevention and not allow it to accumulate, which would be the case for the chaotic structure development. Having both features side by side means that the formation of the structures can switch extremely rapidly and the formation mechanism are competing.

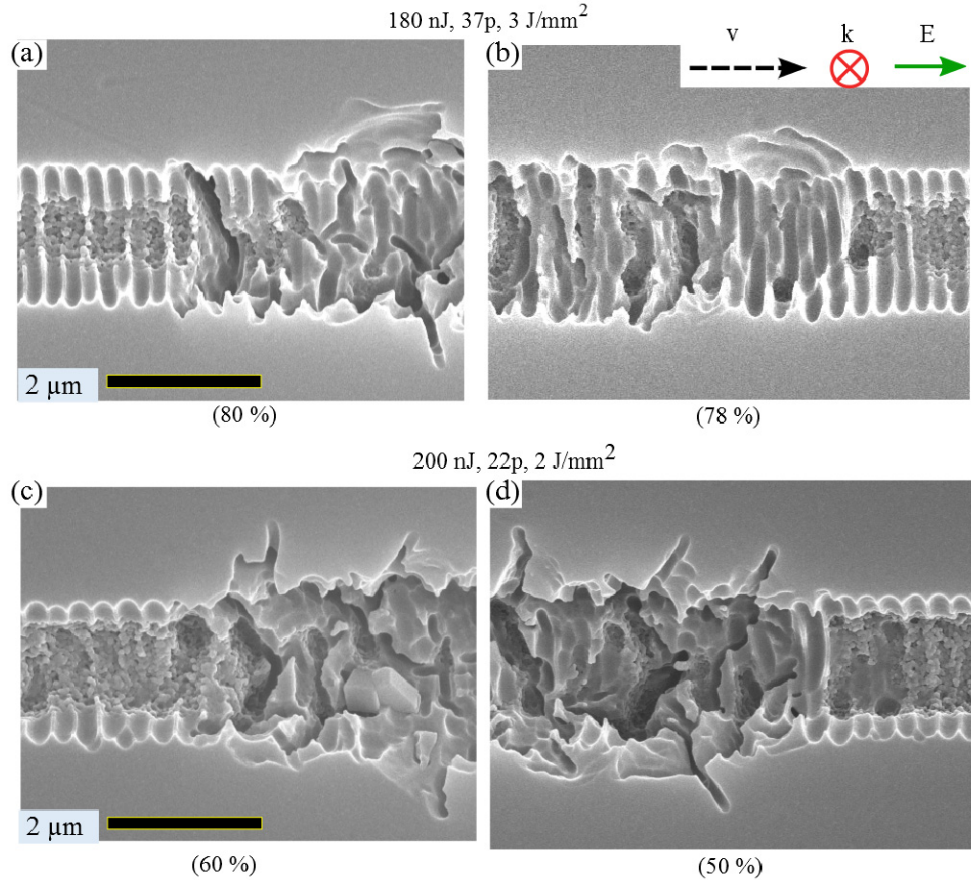


Fig. 7. High magnification images of (a) the transition to disorder, (b) the transition to self-organized nanogratings from the same disordered section that began in (a); and (c) transition to a disordered structure and (d) transitioning back to self-organized again for the same disordered section. The value in the brackets indicates the percentage volume of the LAZ that is below the surface.

2.5 Energy deposition influence on the occurrence of intermittence

As the transitions are linked to accumulated stress, a number of laser-written lines with varying overlapping pulses i.e. energy deposition, were written through the surface of the glass to examine the relationship with the structural transition and to collect some statistical information about the transitions. The resultant structures were examined under the SEM and the positions of the transitions were recorded. Figure 8 summarizes the different structures of the nanogratings within the laser tracks. Three pulse energies were chosen based on previous results of the intermittent behavior. For each pulse energy, the energy deposition was varied between 2 and 10 J/mm² by changing the writing speed (from 30560 μm/s to 6110 μm/s for

180 nJ, 33950 $\mu\text{m/s}$ to 6790 $\mu\text{m/s}$ for 200 nJ and 37350 $\mu\text{m/s}$ to 7470 $\mu\text{m/s}$ for 220 nJ) and therefore changing the number of overlapping pulses. The starting position of the modifications was recorded at the beginning of continuous self-organized patterns or onset of the chaotic structure. The laser tracks are presented in three colors: black indicating regions where only the self-organized structures were present; red for the chaotic structures; and grey, which were self-organized structures that were excluded from the statistical analysis of the laser tracks. 200 μm from the ends of the laser tracks used in the statistical study were excluded to avoid influences from the modifications of the LAZ's tail and tip.

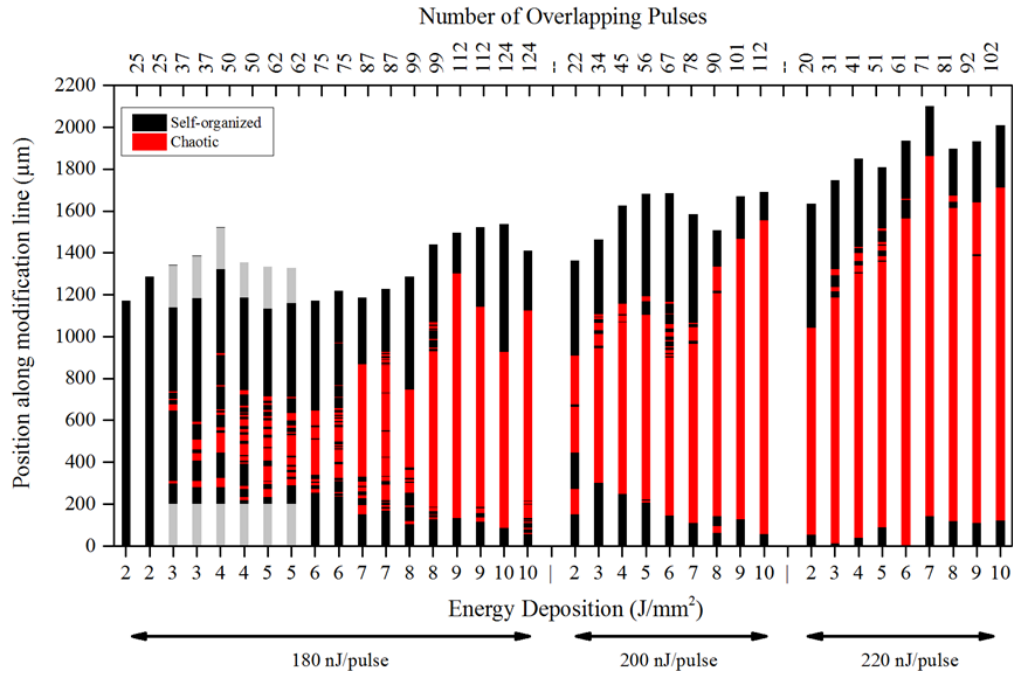


Fig. 8. Overview of the transitions for different energy depositions and pulse energies. Black regions represent the self-organized patterns and red are the chaotic patterns. For the 180 nJ/pulse set, a pair of lines with the same exposure conditions are shown. The light grey shading on the ends of the 3 – 5 J/mm^2 laser tracks signify the zones that were excluded from the statistical analysis in the queueing system section.

As the number of overlapping pulses increased (increasing energy deposition), the length of the chaotic pattern becomes longer. Likewise, the higher pulse energies also show the same trend, i.e. an increase in the length of the chaotic patterns. Eventually the laser tracks are predominantly the chaotic structures for both conditions. In addition, the amount of intermittency is reduced as the pulse energy is increased. To examine the statistical nature of the intermittency, multiple lines were written at 180 nJ/pulse with the same exposure conditions. A comparison of those laser track pairs shows the randomness of the self-organized and chaotic transitioning. It is also clear that the transitions preferentially occur with a larger portion of the LAZ beneath the surface as seen in Fig. 8.

The same modification trend was observed for the specimen with the in-plane tracks for 180 nJ pulse energy (Fig. 9(a)). Both the length of the chaotic region as well as the occurrence frequency has increased with increasing number of pulses. Statistical analysis of the in-plane tracks (detailed in a later section) excluded 500 μm from either end to avoid possible changes due to the specimen's edge or stage deceleration (as the end of the track was not continued beyond the specimen's far edge). The transitions occur across the majority of the laser track's length, although with a noticeable reduction in transitions at the edges of the

tracks for reason that are still unknown as the conditions across the analyzed length were the same. The type of transition that occurred with the in-plane track is virtually identical to that for the inclined track as is expected (Fig. 9(b)).

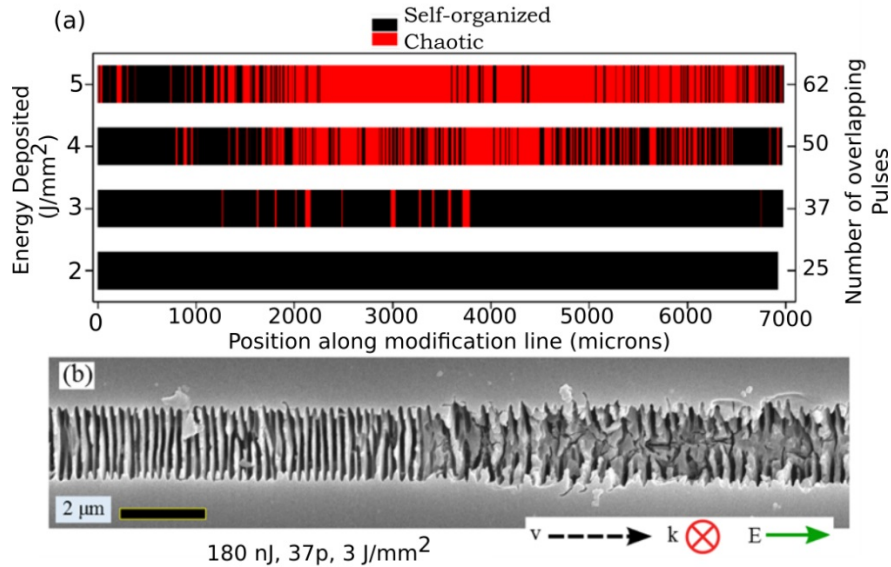


Fig. 9. (a) Overview of the transitions for the in-plane laser tracks of the 2 – 5 J/mm^2 energy depositions for 180 nJ pulse energy. Black regions: self-organized patterns; and red: chaotic patterns. (b) A transition from self-organized to chaotic for the 3 J/mm^2 laser track with approximately $50 \pm 15\%$ of the laser volume below the surface.

3. Physical phenomenological interpretation

3.1 Transition to chaotic from self-organization

We interpret the formation of cracks within the chaotic structure stemming from the self-organized periodic patterns as follows:

- In [10], we have demonstrated that the formation of nan gratings is accompanied by a net volume expansion. This volume expansion is attributed to the formation of a porous structure within lamellae forming the nan gratings. Evidence of the presence of these nanopores inside the lamellae has been reported by J. Canning *et al.* [9].
- Due to the confocal parameters (moderate NA of 0.4), the laser affected zones occupies an ellipsoid volume stretched along the laser propagation axis. If we assume the porosity found in nan gratings is homogeneous (which seems to be the case based on the observations from J. Canning *et al.* [9], later confirmed by Richter *et al.* [15]), considering the shape of the laser affected zones, we do expect high stress concentration to form near pronounced discontinuities, i.e. for instance at the tip of lamellae. Cracks are likely to form in the less dense material or at the interface between the pristine glass and the laser-modified zones. Such localized cracks were observed in [23] using an AFM (atomic force microscope) equipped with a scanning thermal probe. This observation tends to support the proposed model. Furthermore, the surface interface and the presence of localized ablation may act as preferred zones for crack nucleation.
- Lamellae are oriented perpendicular to the writing direction and therefore, the overall stacked-up volume expansion along the writing direction generates significant shear

stress at the interface that can be a source of sliding (commonly referred as mode II cracks) or tearing mode cracks (so-called mode III). This could explain the preferably oblique orientation of the cracks observed in Fig. 7. Such cracks located nearby the interface can eventually propagate inside laser lamellae - being converted from a sliding to an opening mode (referred as mode I). However, due to the presence of compressive stress in between lamellae, when formed, it can hardly propagate across lamellae. Since each lamellae generates compressive stress around it, crack propagation is impeded and thus cannot easily move across lamellae but rather move in a vertical direction with far less obstruction. Indeed, we did not observe any continuous cracks moving across the lamellae. The nanogratings are therefore forming an efficient crack arrest structure preventing cracks from propagating much further than the width of the laser affected zones. It is interesting to notice that this is an unusual behavior in brittle materials where cracks cannot usually be stopped once initiated; it is more akin to ductile material where plastic deformation or grain boundaries can dissipate the crack energy and stop them.

- We did not observe cracks forming in well-defined nanostructures. Immediately after a crack is found, a chaotic sequence is found. This is clearly visible in the examples shown in Fig. 7. This means that cracks form at the time the laser focus is still present. These cracks create interfaces that disturb the propagation of light in the material, alter the heat dissipation in the material as well as the propagation of shock waves and dissipation of shock wave. The shock waves would propagate at the acoustic velocity in glass, ~ 5750 m/s [18, 24]. This overall less effective energy dissipation explains that laser affected zones in chaotic sequences are wider.

3.3 Transition to self-organization from chaotic pattern

The transition from chaotic to self-organized nanostructure ('the self-healing mechanism') could be explained as follows:

- Considering the previous hypothesis and observation that cracks remain confined in a volume that at most barely exceeds the laser affected zones, their interaction with the moving laser focus remains local.
- Cracks initiation is in essence a random process that in glass may be governed by Weibull statistics [25]. Cracks may form randomly in the laser focus and may propagate in the scanning direction or opposite. If a sufficient volume of the material under the laser focus remains crack-free enough to make the formation of organized or partially organized lamellae possible, these lamellae will form a barrier that will stop the cracking process, and eventually restore the possibility for self-organized nanogratings to form.

4. Discussions and interpretations

In what precedes, we have unraveled the occurrence of an intermittent behavior in the formation of self-organized patterns while writing lines at various speed and pulse energies. The system alternates erratically between highly organized and chaotic regimes. This phenomenon is puzzling in many aspects. In this section, we propose a physical interpretation of this behavior. The material used here is high purity one (optical grade with extremely low content of impurities) with a homogeneous structure, albeit glassy. It is therefore unlikely that the observed erratic patterns can be explained by the sole presence of inhomogeneity in the material. The source of energy, the femtosecond laser source, is rather stable energy-wise: pulse energy fluctuates from pulse-to-pulse within less than 5% and there is no long-period pulse energy fluctuation that could be correlated to the typical periodicity of the erratic patterns. Figure 10 shows the fluctuations in laser power during the specimen processing at

the different laser pulse energies. Also shown, is the time duration of actual laser track processing (light green bands) for both the 2 and 10 J/mm² energy depositions (the two extremes) in the approximate location within the overall program execution time to write a series of laser tracks at each pulse energy. It is apparent that the random laser fluctuation is likely to occur at most twice during the laser processing of the highest energy deposition (10 J/mm²) i.e. the longest time duration in laser processing. In short, there is no correlation between the occurrence of the intermittent patterns and measurable laser fluctuations.

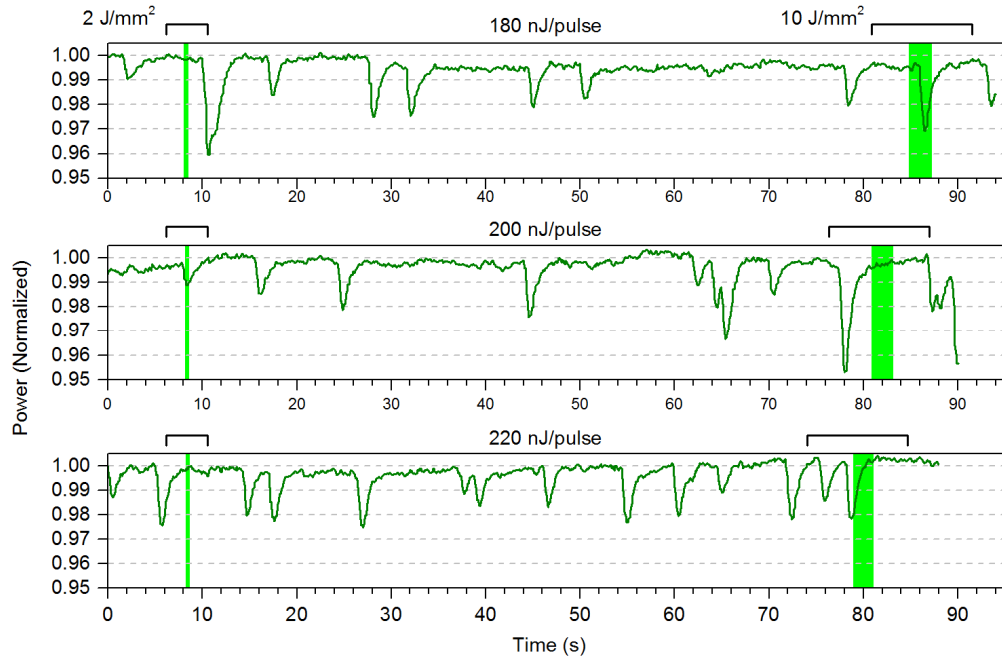


Fig. 10. Laser power fluctuations recording during laser processing of specimen for 180nJ/pulse (top), 200 nJ/pulse (middle) and 220 nJ/pulse (bottom). The light green bands represent the duration of the laser when processing the 2 J/mm² (left) and 10 J/mm² (right) tracks. The exact position of laser track processing (light green bands) was not known precisely and the uncertainty range is shown by the square bracket above the green bands.

Before examining further the physical cause of this intermittent behavior, let us examine the formation process of the regenerative dissipative patterns. To do so, in what follows, we adopt a descriptive point of view directly inspired from queueing theory. This description offers the possibility to extract useful information concerning the dynamics of the system with yet a rather limited amount of experimental information.

4.1 Regenerative intermittent dissipative patterns from the view point of queueing theory

The regenerative alternation between self-organized or **regular R** and chaotic or **erratic E** patterns with random lengths forms statistically independent cycles with random length durations. To progress towards physical explanations, different strategies can be adopted. Instead of a purely microscopic approach which requires a refined understanding of the various processes involved and consecutive to the laser-matter interaction, for the time being, we adopt a phenomenological approach entirely based on an energy dissipation balance. On one hand, the femtosecond laser steadily delivers, via identical and regular periodic pulses, energy to the glass specimen. This energy has to be steadily dissipated into the material via several mechanisms, like reflection, defect formation, recombination mechanism, nano-pores formation, crack formations and most probably several other complementary complex phenomena. While the observed transitions from an **R** to an **E** regime does not really question

too much our intuition, the reverse mechanism which enables the pattern regeneration, is however truly intriguing. The random intermittent alternations between higher configuration entropy (disorganized) to organized patterns with lower entropy is the manifestation of an erratic energy dissipative mechanism which qualitatively is very similar to the behavior of server able to purge a waiting line of customers in a queuing system (see Fig. 11).

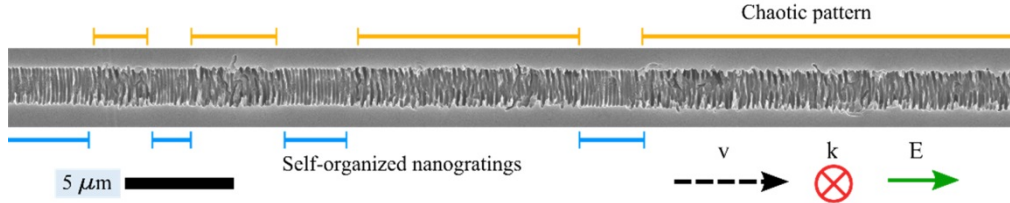


Fig. 11. Typical regenerative pattern observed in a glass specimen scanned by a femtosecond laser with uniform translation velocity. Orange (top) and blue (bottom) bars indicate chaotic and self-organized patterns, respectively.

4 Conclusions and perspectives

The phenomenon of self-organized nanograting formation is an intriguing aspect to ultrashort laser-material interaction. One of the most intriguing findings of this study has been the material's ability to *self-heal* from chaotic to self-organized structures. In addition to the transition, interesting features within the nanogratings have been observed. The sub-microspheres (Fig. 4) show that even though femtosecond excitation processes are typically attributed to non-thermal through direct excitation with the electrons of the material's matrix, there are still thermal processes that can occur, resulting in the formation of the resolidified sub-microspheres. The proximity to the surface has increased the formation of the sub-microspheres. Even though the pulse energy of the laser is considerably low, it is still sufficient to cause minor ablation. Both these features are added material modification structures that need to be carefully considered when producing micromachined devices. Further, the expected alignment of the nanograting lamellae cannot be naturally assumed parallel. Multiple observations (Fig. 2, 3 and 5) of the non-uniformity of the lamellae show that there is a random nature to the formation. Most theories that have been put forth so far do not account for this effect.

This intermittent behavior is bound to the existence of randomness and fluctuations in the process of energy dissipation in the material that finds its origin in the fracture mechanics of the material. The probability of fracture of a glass material under a given stress has been described using Weibull statistical law [25]. In this context, the cumulative probability for the glass to fracture at a given stress σ is formulated in its general form as followed:

$$P(\sigma) = 1 - \exp \left[- \left(\frac{\sigma}{\sigma_N} \right)^m \right]$$

The function is defined by two parameters: a nominal stress σ_N and an exponential factor m . Both parameters are determined experimentally by fitting an experimental curve in a log-log plots derived from Eq. (13). This approach requires performing numerous experiments, which is cumbersome and fastidious.

Here, the formation of individual elements of a pattern could be seen as a single loading experiment that are, in first approximation, independent from the previous experiments. Therefore, the number of patterns formed before observing an actual fracture of the system provides a measurement of the probability for fracture and as such, possible data points for determining σ_N and the exponential factor for the m . This method has the potential to offer a fast method for determining Weibull parameters.

Acknowledgment

This project is supported by the European Research Council (ERC Stg Galatea - 307442).